Dynamic Responses of Child Occupant in Side Impact

YANG Xingmei, YANG Jikuang, JIANG Xiaoqing
State Key Laboratory of Advanced Design and Manufacturing for Vehicle Body,
Research Center of Vehicle & Traffic Safety, Hunan University, Changsha, 410082, yang_xingmei2003@yahoo.com.cn

Abstract: The paper describes the study of dynamic responses of restrained child occupant in side impact. In order to obtain the dynamic deformation of side structures of the car during side collision, which can influence these dynamic responses, the model of two vehicles was used in simulations of the three different impact angles and impact velocities in LS-Dyna program. Based on the model of impacted vehicle represented in LS-Dyna, the model of vehicle structures was developed in MADYMO environment and combined with P6 child dummy. To simulate the dynamic deformation of the door, the Prescribed Structure Motion (PSM) method was used. The head acceleration, thorax acceleration, neck force and moment of the child dummy were calculated and compared in simulations of three impact angles and velocities of the side impact. The results confirmed that the impact velocity has big effect on the resultant head acceleration, resultant thorax acceleration, neck force in z-direction and neck moment around y-axis. All maximum values of these parameters, except the resultant thorax acceleration, increased with the increase of impact velocity. For various impact angles, the resultant thorax acceleration did not present certain trend in relation to the impact velocities. For various impact velocities, the resultant head acceleration, resultant thorax acceleration, neck force in z-direction and neck moment around y-axis did not present certain trend in relation to the impact angles and were influenced mainly by dynamic deformation of the side structures of the vehicle. The study shows the importance to consider the dynamic deformation of the vehicle structures in evaluation of the protective effect of child restraint systems.
Keywords: Side impact, Child occupant, CRS, Dynamic response, PSM

1 Introduction

The side impact is dangerous to child occupants, especially in near impact side position [1-4]. According to the report from NHTSA [5] in 1999 in USA, 1,317 children between the ages of 0 to 12 have been killed in motor vehicle crashes and 31.89% of them were involved in side impact crashes. Of these, children seated on the near impact side position represent 55% of the fatalities. Canadian data from side impact accidents confirms that the near impact side position is the most dangerous one in the vehicle. Moreover, the vehicle body intrusion is very important especially when the CRS is positioned on the nearside to the impact area [6]. In China, the data of Changsha Traffic Police Accident Database indicate that from 2001 to 2006 the side impact accounts for 45% of accidents involved injured 0-15 year old child occupant [7].

At present, there is not uniform side impact test procedure for CRS. ISO/TC22/SC12 WG1 (working group on child safety inside passenger cars) is developing a side impact test procedure for CRS, taking into account other side impact test procedures for CRS already implemented in some countries. The proposed side impact test method for CRS according to ISO DIS 14646 reproduces vehicle acceleration by a sled and intrusion by a hinged panel. Based on full-car side impact tests, a corridor of the sled delta-V and the panel angular velocity is prescribed [8].

Recently the protection of children by CRS in side collisions was evaluated in several studies, most of them are about 0-3 year old child occupants. For example, Surcel and Gou [9] studied the dynamic responses of Hybrid III 3 year old dummy in 90º side impact and two impact speeds 33.8 km/h and 62.1 km/h. They pointed out that the door intrusion has big influence on the HIC that is directly proportional to the impact speed. However the door intrusion has little influence on the thorax acceleration. In order to simulate the responses of Q3s and CRABI 6-month-old dummy protected by CRS, Hu and Mizuno [10] performed sled tests based on the ISO side impact test procedure. They emphasized that the load on the thorax of child dummy in forward or rearward child safety seat is mainly caused by the door intrusion.

However, the dynamic responses of 4-8 year old child occupant restrained in booster seat are not clear. Otte [11] studied the side impact accident data in Germany form 1985 to 2001. He found that the head, neck, thorax and extremities are frequently injured. As most of the injury to the extremities is not threat to life, most of the injury to head, neck and thorax is serious and these regions should be protected firstly. Therefore the dynamic responses of head, neck and thorax of P6 child dummy restrained in booster seat were evaluated for various impact angles and velocities. Because most of children are placed in the rear seat we decided to simulate the impact to rear door of the struck vehicle.

2 Materials and Methods

2.1 LS-Dyna Simulation

In the side impact the dynamic deformation of door is an important parameter influencing the risk of injuries. This side deformation we obtained from LS-Dyna simulations. The impact model of two vehicles was developed using LS-Dyna program, see Figure 1. The impact to the rear door of the struck vehicle was simulated. The velocities of the striking vehicle were 30 km/h, 50 km/h and 70 km/h and they represent the low, middle and high velocity. The struck vehicle was stationary. The impact angles of the striking car were 30º, 60º and 90º with respect to the struck vehicle. Nagabhushana et al.[12] studied the accident data about child occupants aged from 1 to 8 in nearside impact position from NASS/CDS database and found that 90% of side impact accidents are in configuration between 30º and 90º. In these accidents 56% of injury can be found when the primary direction of force (PDOF) is about 60º. The definition of impact angle is shown in Figure 2. These impact angles selected represent most of the side impacts. The same model was used for the striking and struck vehicle. This model was previously validated in side impacts [13]. The mass of the vehicle model was 1,170.5 kg. The number of nodes and elements of this model was 339,622 and 337,750 respectively.

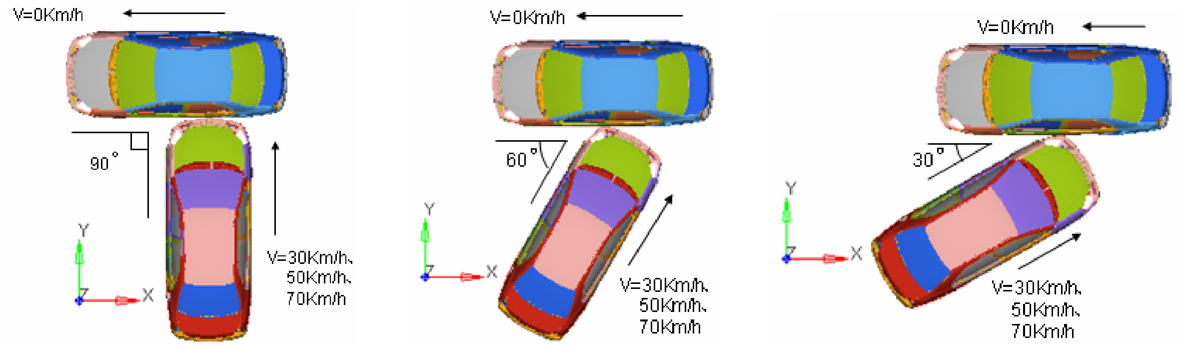

Figure 1. The configuration of impact model of two vehicles

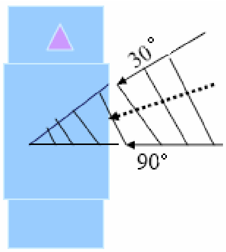

Figure 2. The impact angle in side impact collision, based on [12]

2.2 MADYMO Simulation

To evaluate the dynamic responses of head, neck and thorax of the child dummy we used the MADYMO software. The simulation model comprised the P6 dummy, booster seat, side structure and vehicle rear seat including the safety belt system. The P6 dummy model was taken from MADYMO 6.2.1 database. The booster seat model was developed with Geomagic software based on Anbel C21 booster seat that is manufactured by Shenzhen Abel Auto Accessory Co. Ltd. This booster seat is common in the market. The substructure prescribed motion from full vehicle analysis (PSM method) was used to simulate the dynamic deformation of door. This method is effective when computing time is considered. The geometry of the vehicle seat model was described by two ellipsoids that represent the seat base and seat back. The three-point belt system was a hybrid type. It consists of FE shell elements, while the ends were modeled by non-linear elastic springs. The components of motion of center of gravity (c.o.g.) of vehicle body from the LS-Dyna simulation were used in the MADYMO simulation. The combination of three impact angles and velocities of side impact were simulated according to the test matrix presented in Table 1. As the indicator of injury risk we selected in the all simulations to analyze the time history of head acceleration, thorax acceleration, and force and moment on the neck.

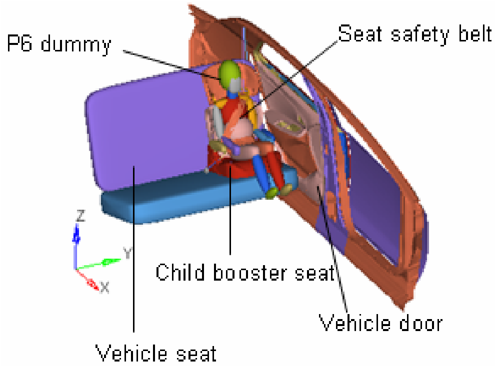

Figure 3 The simulation model in MADYMO program

Table 1. The combinations of three impact angles and velocities of side impact

Simulation	Type of CRS	Impact angle [º]	Impact Velocity [km/h]
S 1	Belt-positioning booster seat	90	30
S 2		90	50
S 3		90	70
S 4		60	30
S 5		60	50
S 6		60	70
S 7		30	30
S 8		30	50
S 9		30	70

3 Results

3.1 Motion components and door dynamic deformation

The motion of vehicle in real world is composed of the translations in x-, y- and z-direction and roll, pitch, and yaw. As the injuries of child occupant are mainly caused from the impact in XY-plane, the simulation results in XY-plane were considered. The motions components of c.o.g. of the stuck vehicle are presented in Figure 4.

The dynamic deformations of the door of struck vehicle in all simulations are presented in Figure 5.

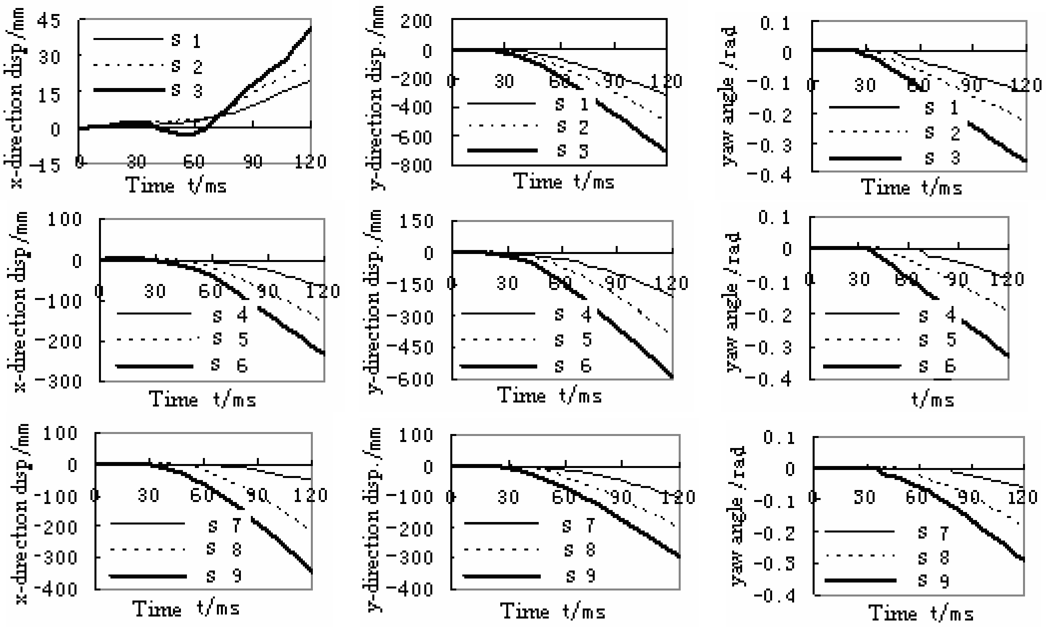

Figure 4. The displacement in x- and y- direction and the yaw angle in z-direction of c.o.g. of the struck vehicle from nine simulations

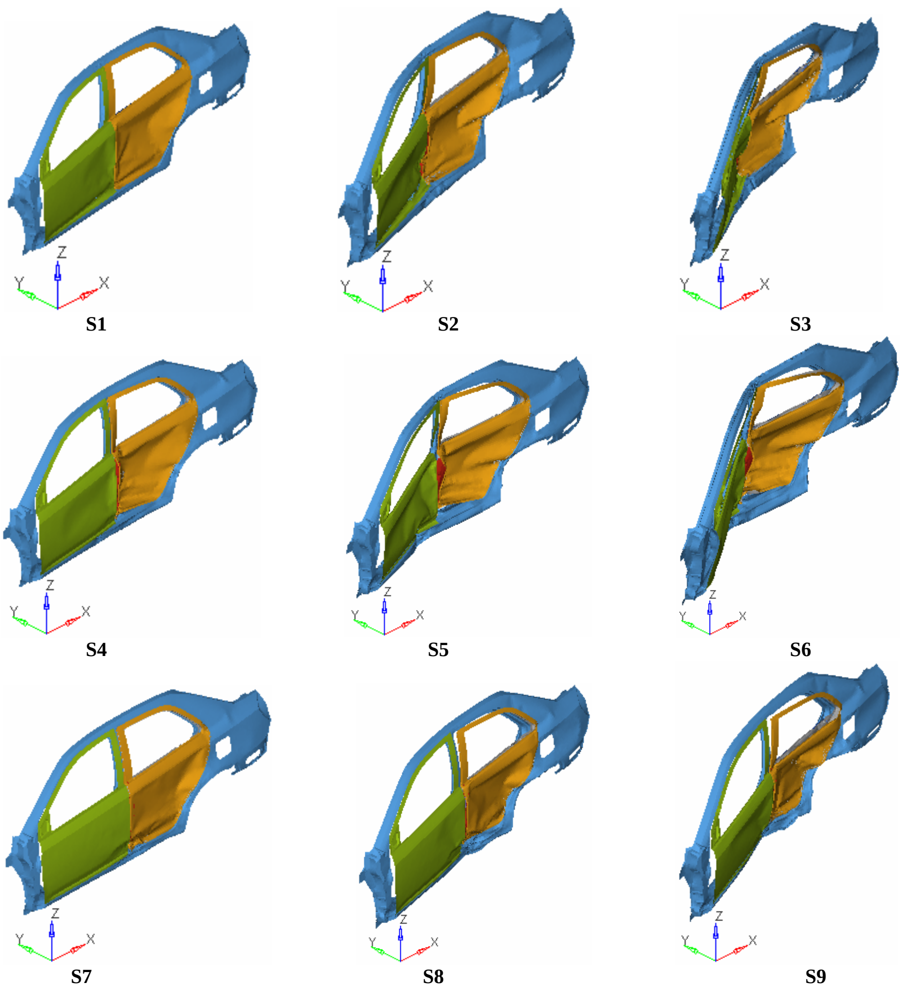

Figure 5. The dynamic deformation of the door of the struck vehicle from nine simulations (ISO view)

3.2 Dynamic response of the child dummy

3.2.1 Impact angle of 90°

In the first analysis performed in the study we compared dummy dynamic response at certain impact angle. The Figure 6 summarizes the time histories of dynamic responses of the head, thorax and neck when the impact angle is 90º. In Figure 6 (a) we can see that with the increase of the impact velocity, the maximum value of the resultant head acceleration also increases. When the impact velocity is high, the maximum value of this acceleration appears earlier than in case of low velocity. In simulation S1 the maximum value of the resultant head acceleration 70 g appears at 66.5 ms. In simulation S2 the maximum value of 310 g, which increased about 340% in relation to that in simulation S1, appears at 38.8 ms. In simulation S3 the maximum value of 870 g, which increased more than ten times in relation to that in simulation S1, appears at 32 ms. In the three simulations the increase of the head acceleration is in relation to the velocity and the maximum value occurs when the intruding door trim impacted the booster seat and caused the impact of dummy head to the headrest of booster seat.

From Figure 6 (b) we can see that in simulation S1 the maximum value of the resultant thorax acceleration (130 g) appears at 55.4 ms. In simulation S2 the maximum value of the acceleration of 630 g, increased so much as 380% in relation to that in simulation S1, appears at 44.7 ms. In simulation S3 the maximum value of the acceleration of 460 g, increased only about 250% in relation to that in simulation S1, appears at 29.4 ms. In the three simulations the time occurrence of maximum value of thorax acceleration is influenced mainly by two aspects. One is the intruding door trim impact to the dummy upper torso; the other is the restraint force developed between shoulder belt and the upper torso of dummy.

Figure 6 (c) and 6 (d) indicate that the dummy neck force in z-direction and moment around y-axis increase with the increase of impact velocity. The maximum value of the neck force z-direction (-1305 N) appears at 72.3 ms and the maximum value of the moment around y-axis (-7 Nm) appears at 66 ms in simulation S1. In simulation S2 the maximum value of the force of 8424 N, increased about 540% in relation to that in simulation S1, and the maximum value of the moment of -61 Nm, increased about 770% in relation to that in simulation S1, appears at 39 ms. In simulation S3 the maximum value of the force of 24643 N, increased about 17 times in relation to that in simulation S1, and the maximum value of the moment of -157 Nm, increased about 20 times in relation to that in simulation S1, appears at 32.1 ms. The dummy neck force and moment are caused by the motion of the head in relation to thorax.

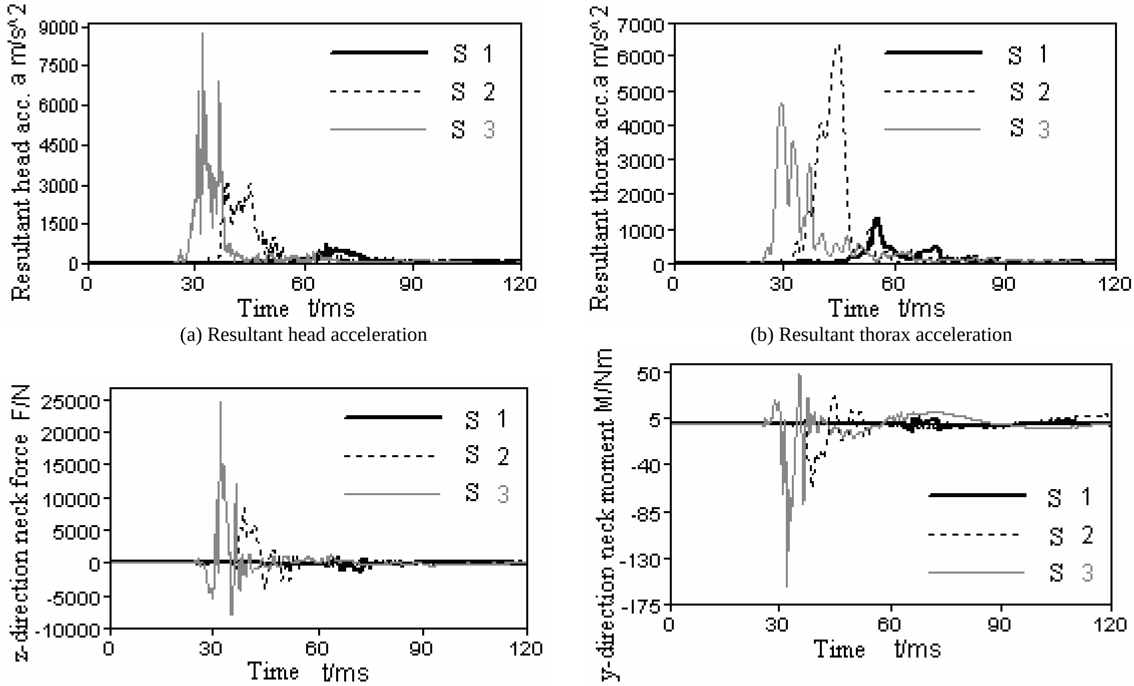

(a) Resultant head acceleration (b) Resultant thorax acceleration

(c) Neck force in z-direction (d) Neck moment around y-axis

Figure 6. Dynamic responses of the dummy – impact angle 90º

3.2.2 Impact angle of 60°

The Figure 7 summarizes the time histories of dynamic responses of the head, thorax and neck when the impact angle is 60º. In Figure 7 (a), one can see that with the increase of the impact velocity, the maximum value of the resultant head acceleration also increases. When this velocity is high, the time occurrence of maximum value of head acceleration is earlier than for low velocity. In simulation S4 the maximum value of the resultant head acceleration (88 g) appears at 87.3 ms. In simulation S5 the maximum value of the acceleration of 282 g, increased about 220% in relation to that in simulation S4, appears at 50.5 ms. In simulation S6 the maximum value of the acceleration of 616g, increased about 600% in relation to that in simulation S4, appears at 40.5 ms. In the three simulations of impact angle of 60º, the increase of the head acceleration is also in relation to the velocity and the maximum value occurs, similarly as in simulation of 90º impact, when the intruding door trim impacted the booster seat and caused the impact of dummy head to the headrest of booster seat.

From Figure 7 (b) we can see that with the increase of the impact velocity, the maximum value of the resultant thorax acceleration also increases. When the velocity is high, the time occurrence of maximum value of thorax acceleration is earlier than for low velocity. In simulation S4 the maximum value of the resultant thorax acceleration (87 g) appears at 87.9 ms. In simulation S5 the maximum value of the acceleration of 344 g, increased about 290% in relation to that in simulation S4, appears at 51.3 ms. In simulation S6 the maximum value of the acceleration of 746 g, increased about 750% in relation to that in simulation S4, appears at 40.5 ms. Similarly to the simulation of 90º impact in the three simulations the time occurrence of maximum value of thorax acceleration is also influenced mainly by two aspects: door trim impact to the dummy and the restraint force developed.

Figure 7 (c) and 7 (d) indicate that the dummy neck force in z-direction and moment around y-axis increase with the increased impact velocity. In simulation S4 the maximum value of the neck force in z-direction (2661 N) and the maximum value of the moment around y-axis (-19 Nm) appears at 88 ms. In simulation S5 the maximum value of force of 5668 N, increased about 110% in relation to that in simulation S4, and the maximum value of the moment of -38 Nm, increased about 100% in relation to that in simulation S4, appears at 50.5 ms. In simulation S6 the maximum value of force of -17106 N, increased about 540% in relation to that in simulation S4, and the maximum value of the moment of 103 Nm, increased about 440% in relation to that in simulation S4, appears at 40.4 ms. Similarly to the impact in 90º configuration, the dummy neck force and moment are caused by the motion of the head in relation the thorax.

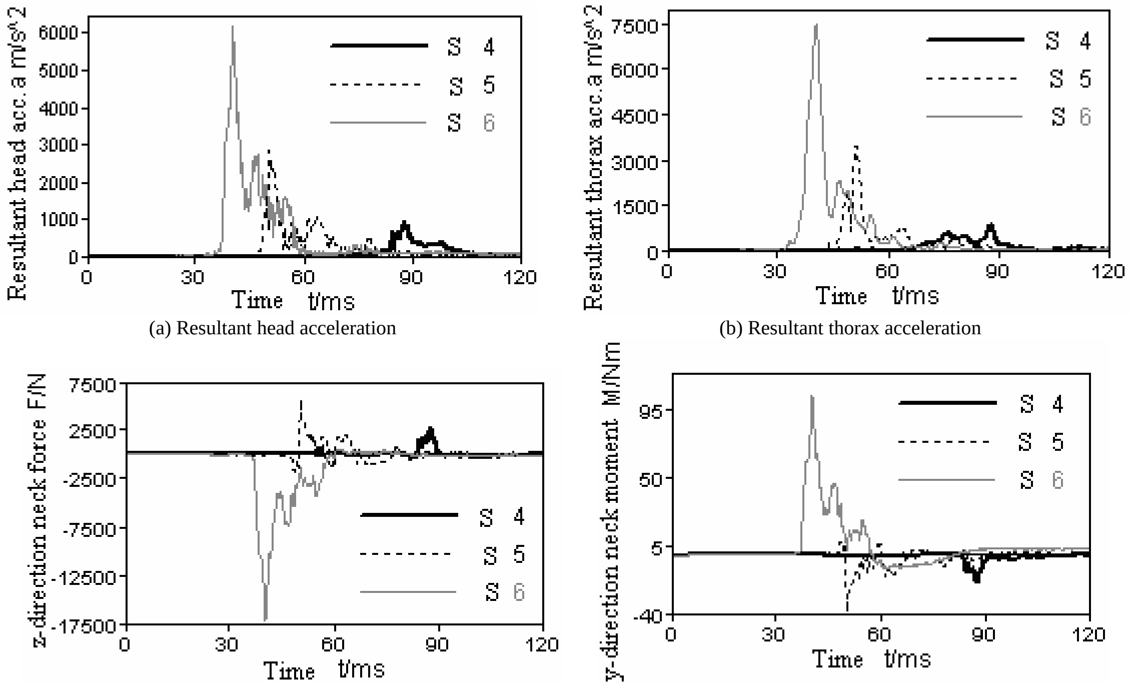

(a) Resultant head acceleration (b) Resultant thorax acceleration

(c) Neck force in z-direction (d) Neck moment around y-axis

Figure 7. Dynamic responses of the dummy – impact angle 60º

3. 2.3 Impact angle of 30°

The Figure 8 summarizes the time histories of dynamic responses of the head, thorax and neck when the impact angle is 30º. In Figure 8 (a) one can see that with the increase of the impact velocity, the maximum value of the resultant head acceleration also increases. Similarly to the results from simulations of the 90º and 60º impacts, when this velocity is high, the time occurrence of maximum value of head acceleration is earlier than for low velocity. In simulation S7 the maximum value of the resultant head acceleration (17 g) appears at 112.2 ms. In simulation S8 the value of 76 g, increased about 350% in relation to that in simulation S7, appears at 72.7 ms. In simulation S9 the value of 506 g, increased about 28 times in relation to that in simulation S7, appears at 56.6 ms. In the three simulations of impact angle of 30º, the increase of the head acceleration is also in relation to the velocity and the maximum value occurs, similarly as in simulation of 90º and 60º impacts, when the intruding door trim impacted the booster seat and caused the impact of dummy head to the headrest of booster seat.

From Figure 8 (b) we can see that the maximum value of the resultant thorax acceleration also increases with the increasing of the impact velocity. Similarly as in simulation of 90º and 60º when the velocity is high, the time occurrence of maximum value of thorax acceleration is earlier than for low velocity. In simulation S7 the maximum value of the resultant thorax acceleration (19 g) appears at 79.3 ms. In simulation S8 the value of 130 g, increased about 580% in relation to that in simulation S7, appears at 68.3 ms. In simulation S9 the value of 743 g, increased about 38 times in relation to that in simulation S7, appears at 56.4 ms. Similarly to the simulation of 90º and 60º impacts in the three simulations the time occurrence of maximum value of thorax acceleration is also influenced mainly by two aspects: door trim impact to the dummy and the restraint force developed.

Figure 8 (c) and 8 (d) indicate that also in 30º configuration the neck force in z-direction and moment around y-axis increase with the increasing impact velocity. In simulation S7 the maximum value of the neck force in z-direction (-357 N) appears at 80 ms and the maximum value of the moment around y-axis (-5 Nm) appears at 118.2 ms. In simulation S8 the value of 2345 N, increased about 560% in relation to that in simulation S7, and the value of -13 Nm, increased about 160% in relation to that in simulation S7, appears at 73.6 ms. In simulation S9 the maximum value of-14834 N, increased about 40 times in relation to that in simulation S7, and the value of 96 Nm, increased about 18 times in relation to that in simulation S7, appears at 56.6 ms. Similarly to the impact in 90º and 60º configurations, the dummy neck force and moment are caused by the motion of the head in relation the thorax.

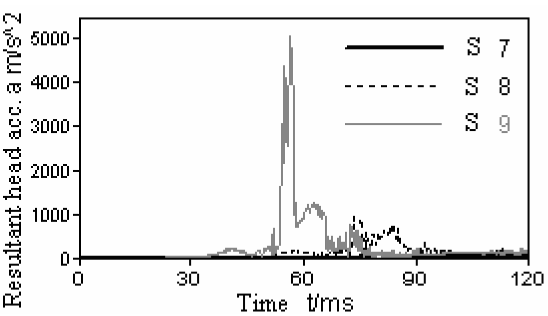

(a) Resultant head acceleration

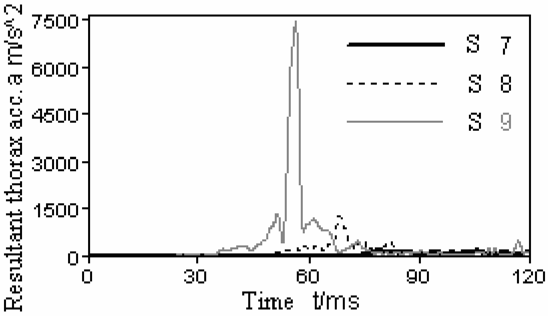

(b) Resultant thorax acceleration

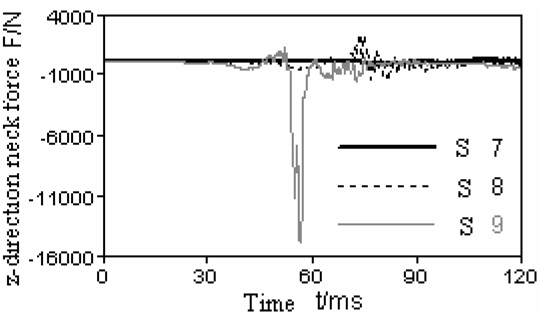

(c) Neck force in z-direction

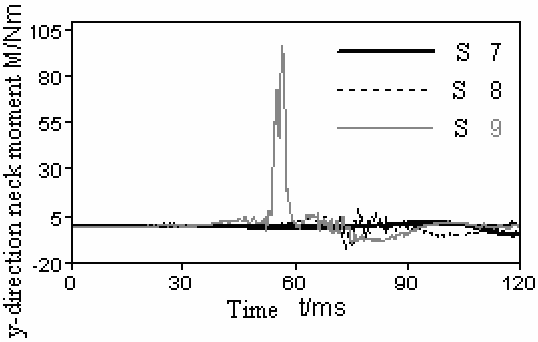

(d) Neck moment around y-axis

Figure 8. Dynamic responses of the dummy – impact angle 30°

3.2. 4 Impact velocity of 30 km/h

In the second analysis performed in the study we compared dummy dynamic responses at certain velocity. The Figure 9 summarizes the time histories of dynamic responses of the head, thorax and neck when the impact velocity is 30 km/h. Figure 9 (a) shows that in simulation S1 the maximum value of resultant head acceleration (70 g) appears at 66.5 ms, in simulation S4 the value of 88 g, increased about 26% in relation to that in simulation S1, appears at 87.3 ms, and in simulation S 7 the value of 17 g, decreased about 76 % in relation to that in simulation S1 appears at 112.2 ms. The order of the resultant head acceleration from high to low is: simulation S4>simulation S1>simulation S7.

Figure 9 (b) shows that in simulation S1 the maximum value of resultant thorax acceleration (130 g) appears at 55.4 ms, in simulation S4 the value of 87 g, decreased about 33% in relation to that in simulation S1, appears at 87.9 ms, and in simulation S7 the value of 19 g, decreased about 85% in relation to that in simulation S1 appears at 79.3 ms. The order of the resultant thorax acceleration from high to low is: simulation S1>simulation S4>simulation S7.

In Figure 9 (c) one can see that in simulation S1 the maximum value of neck force in z-direction (-1305 N) appears at 72.3 ms, in simulation S4 the value of 2661 N, increased about 100% in relation to that in simulation S1, appears at 88 ms, and in simulation S7 the value of -357 N, decreased about 70% in relation to that in simulation S1, appears at 80 ms. The order of the neck force in z-direction from high to low is: simulation S4>simulation S1>simulation S7.

Figure 9 (d) shows that in simulation S1 the maximum value of neck moment around y-axis (-7 Nm) appears at 66 ms, in simulation S4 the value of -19 Nm, increased about 170% in relation to that in simulation S1, appears at 88 ms, and in simulation S7 the value of -5 Nm, decreased about 30% in relation to that in simulation S1, appears at 118.2 ms. The order of the neck force in z-direction from high to low is: simulation S4>simulation S1>simulation S7.

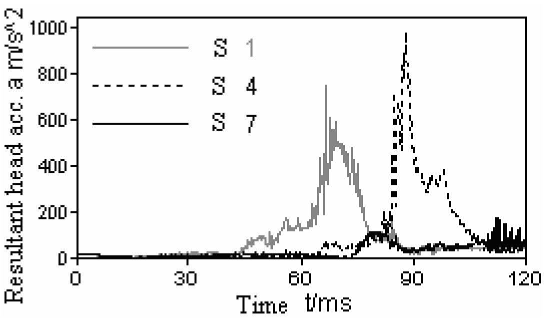

(a) Resultant head acceleration

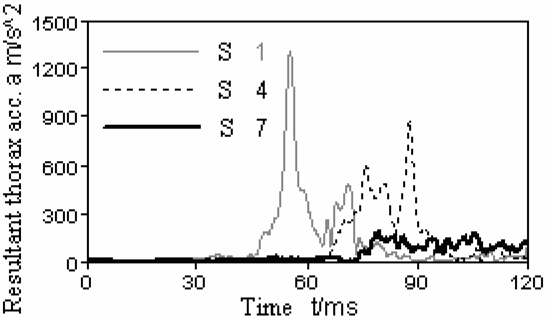

(b) Resultant thorax acceleration

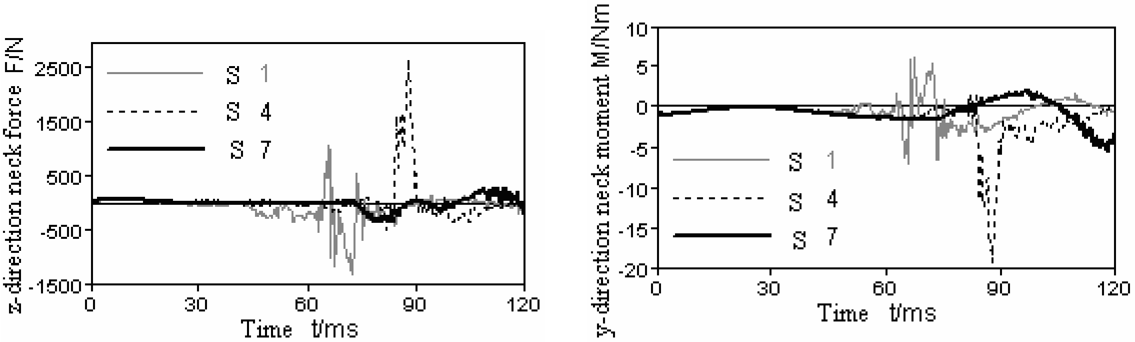

(c) Neck force in z-direction (d) Neck moment around y-axis

Figure 9. Dynamic responses of the dummy – impact velocity 30 km/h

3. 2.5 Impact velocity of 50 km/h

The Figure 10 summarizes the time histories of dynamic responses of the head, thorax and neck when the impact velocity is 50 km/h. In Figure 10 (a) we can see that in simulation S2 the maximum value of resultant head acceleration (310 g) appears at 38.8 ms. In simulation S5 the value of 282 g, decreased about 9% in relation to that in simulation S2, appears at 50.5 ms, and in simulation S8 the value of 76 g, decreased about 75% in relation to that in simulation S2, appears at 72.7 ms. The order of the resultant head acceleration from high to low is: simulation S2>simulation S5>simulation S8.

In Figure 10 (b) one can see that in simulation S2 the maximum value of resultant thorax acceleration (630 g) appears at 44.7 ms, in simulation S5 the value of 344 g, decreased about 45% in relation to that in simulation S2, appears at 51.3 ms, and in simulation S8 the value of 130 g, decreased about 80% in relation to that in simulation S2, appears at 68.3 ms. The order of the resultant thorax acceleration from high to low is: simulation S2>simulation S5>simulation S8.

Figure 10 (c) shows that in simulation S2 the maximum value of neck force in z-direction (8424 N) appears at 39 ms, in simulation S5 the value of 5668 N, decreased about 30% in relation to that in simulation S2, appears at 50.5 ms, and in simulation S8 the value of 2345 N, decreased about 70% in relation to that in simulation S2, appears at 73.6 ms. The order of the neck force in z-direction from high to low is: simulation S2>simulation S5>simulation S8.

In Figure 10 (d) we can see that in simulation S2 the maximum value of neck moment around y-axis (-61 Nm) appears at 39 ms, in simulation S5 the value of -38 Nm, decreased about 40% in relation to that in simulation S2, appears at 50.5 ms, and in simulation S8 the value of -13 Nm, decreased about 80% in relation to that in simulation S2, appears at 73.6 ms. The order of the neck moment around y-axis from high to low is: simulation S2>simulation S5>simulation S8.

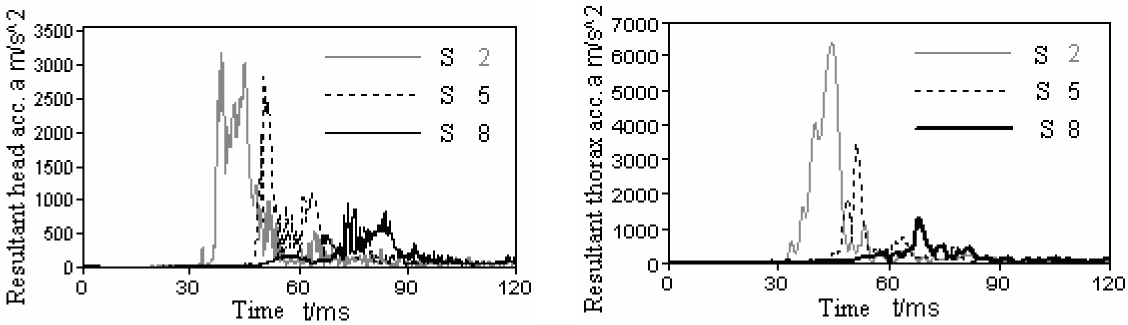

(a) Resultant head acceleration (b) Resultant thorax acceleration

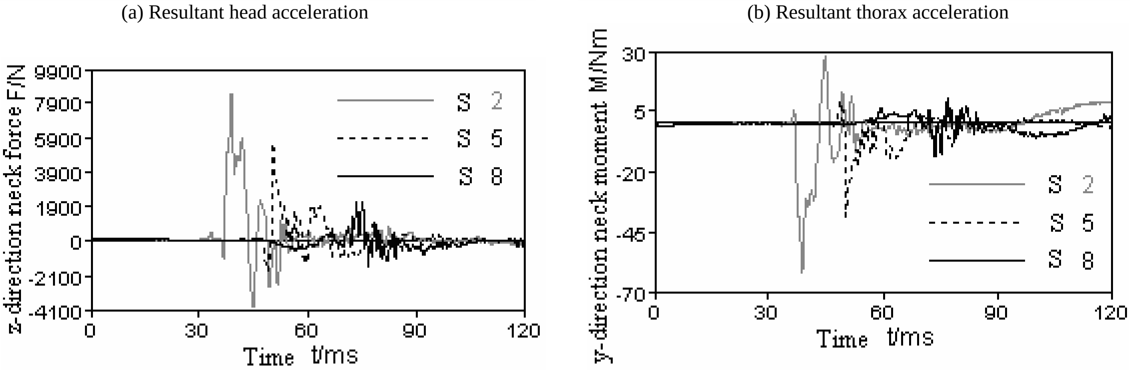

(c) Neck force in z-direction (d) Neck moment around y-axis

Figure 10. Dynamic responses of the dummy – impact velocity 50 km/h

3.2. 6 Impact velocity of 70 km/h

The Figure 11 summarizes the time histories of dynamic responses of the head, thorax and neck when the impact velocity is 70 km/h. In Figure 11 (a) can be found that in simulation S3 the maximum value of resultant head acceleration (870 g) appears at 32 ms, in simulation S6 the value of 616 g, decreased about 30% in relation to that in simulation S3, appears at 40.5 ms, and in simulation S9 the value of 506 g, decreased about 40% in relation to that in simulation S3, appears at 56.6 ms. The order of the resultant head acceleration from high to low is: simulation S3>simulation S6>simulation S9.

Figure 11 (b) shows that in simulation S3 the maximum value of resultant thorax acceleration (460 g) appears at 29.4 ms, in simulation S6 the value of 746 g, increased about 60% in relation to that in simulation S3, appears at 40.5 ms, and in simulation S9 the value of 743 g, increased about 60% in relation to that in simulation S3, appears at 56.4 ms. The order of the resultant thorax acceleration from high to low is: simulation S6>simulation S9>simulation S3.

In Figure 11 (c) is shown that in simulation S3 the maximum value of neck force in z-direction (24643 N) appears at 32.1 ms, in simulation S6 the value of -17106 N, decreased about 30% in relation to that in simulation S3, appears at 40.4 ms, and in simulation S9 the value of -14834 N, decreased about 40% in relation to that in simulation S3, appears at 56.6 ms. The order of the neck force in z-direction from high to low is: simulation S3>simulation S6>simulation S9.

Figure 11 (d) shows that in simulation S3 the maximum value of neck moment around y-axis (-157 Nm) appears at 32.1 ms, in simulation S6 the value of 103 Nm, decreased about 30% in relation to that in simulation S3, appears at 40.4 ms, and finally in simulation S9 the value of 96 Nm, decreased about 40% in relation to that in simulation S3, appears at 56.6 ms. The order of the neck moment around y-axis from high to low is: simulation S3>simulation S6>simulation S9.

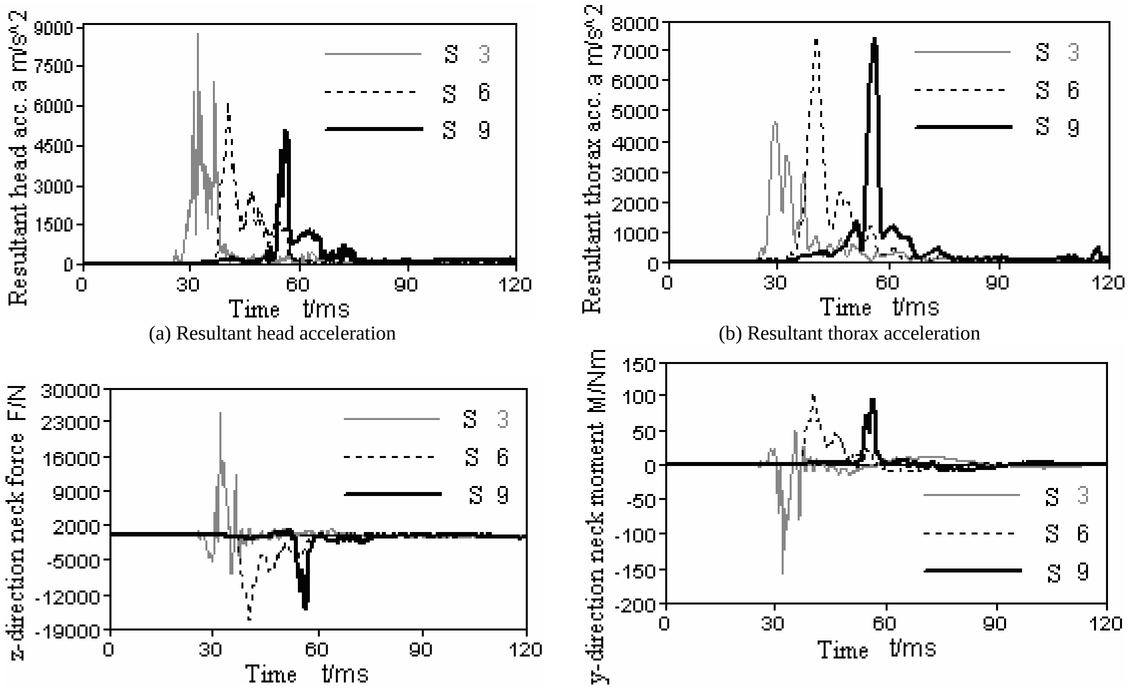

(a) Resultant head acceleration (b) Resultant thorax acceleration

(c) Neck force in z-direction (d) Neck moment around y-axis

Figure 11. Dynamic responses of the dummy – impact velocity 70 km/h

4 Discussions

In the all simulations of side impact the dummy head contacted the headrest of booster seat only. It seems that simulated booster seat could protect the head from impact by the other car structures as the door or window. Consequently, the head injury risk can be reduced by improvement of the energy absorption of headrest material or reduction of the head motion. We found also that in all simulations it was the intruding door trim that impacted the upper torso of dummy. Therefore, increase of the depth of the side wing of booster seat or improvement of its energy absorption can reduce the thorax injury risks.

Regarding the influence of the velocity on the time occurrence of the maximum values of all parameters describing the dynamic response of child dummy we can say that there was a clear trend: the increase of velocity caused early peaks of studied parameters.

Regarding the influence of the dynamic deformation of car structures the situation is complex. Based on the simple theoretical analysis we could expect the proportional effect on dynamic dummy response in relation to vector of impact velocity (amount of velocity and direction). According to this we could find that in all impact configurations, the maximum values of resultant head acceleration, neck force in z-direction and neck moment around y-axis increased with the increase of impact velocity. All these parameters at high velocity increased over 100% in relation to low velocity.

However, due to the accurate method of calculation of dynamic deformation of car structures in LS-Dyna, we could find that this deformation was not uniform and affected the dynamic response of child dummy. For example, when the impact angle was 90º and impact velocity 50 km/h, the maximum value of the resultant thorax acceleration was higher than that at impact velocity of 70 km/h. The reason might be that the dummy upper torso was pushed in y-direction more rapidly by the intrusion of door trim at the impact velocity of 70 km/h than that at impact velocity of 50 km/h. When the impact velocity was 30 km/h and impact angle 60º, the maximum values of resultant head acceleration, neck force in z-direction and neck moment around y-axis were higher than these at impact angle of 90º. The reason might be that the x-component of motion of head at the impact angle of 60º was obviously higher than that at the impact angle of 90º when the impact velocity was low. When the impact velocity was 70 km/h, the maximum values of resultant thorax acceleration at the impact angles of 60º and 30º were at similar level and higher than that at impact angle of 90º. The reason of this situation might be the particular intrusion of door trim at impact angles of 60º and 30º when the impact energy is high. In these configurations we can see extensive deformations of side structures including B-pillar and local deformation of mid-section of rear door, respectively.

5 Conclusions

The impact velocity has big influence on the resultant head acceleration, neck fore in z-direction and neck moment around y-axis than impact angle. The maximum values of these parameters will increase with the increase of impact velocity.

With the change of impact angle, the influences of impact velocity on the resultant thorax acceleration don't present certain trend. This parameter is influenced by the dynamic deformation of the car side structures.

The influences of impact angle on the resultant head acceleration, resultant thorax acceleration, neck force in z-direction and neck moment around y-axis don't present certain trend. These parameters are also influenced by the dynamic deformation of the car side structures.

The current study shows the importance to consider real dynamic deformation of the side structures when discussing the child dummy dynamic response because this deformation can be different from the theoretical one and have a particular influence on the dummy response. Discussing this with other terminology—it correlates with the safety of the child occupants.

The results from the study can be used as guidelines in designing process of child protection systems in side impact collisions. However, to evaluate the protection level of the child occupant in the certain child seat placed in the certain car the use of the methodology from current study can be valuable.

Acknowledgements

The study is sponsored by the National "863 Program" No. 2006AA110101, the Ministry of Education of China "111 program" No. 111-2-11, the Ministry of Education of China "The Program for Changjiang Scholars and Innovative Research Team in University (PCSIRT)" No. 531105050037, and the Autonomous subject Program of the State Key Laboratory of Advanced Design and Manufacturing for Vehicle Body, Hunan University No. 60870004.

References

[1] Langwieder K., Hell W., Willson, H. (1996). Performance of Child Restraint Systems in Real-Life Lateral Collisions. 40th STAPP Car Crash Conference.

[2] Filders B., Charlton J., Fitzharris M., Langwieder K., Hummel T. (2003). Injuries to Children in Child Restraints. Int.J. Crashworthiness, Vol. 8, pp.277–284.

[3] Arbogast K.B., Chen I., Durbin D.R,. Winston F.K. (2004). Injury Risks for Children in Child Restraint Systems in Side Impact Crashes. IRCOBI Conference. Graz, Austria.

[4] Arbogast K.B., Yoganandan G., Menon R.A., Tylko S. (2005). Field Investigation of Child Restraint Systems in Side Impact Crashes. Traffic Injury Prevention, Vol. 6, pp.351–360.

[5] National Highway Traffic Safety Administration, Office of Regulatory Analysis and Evaluation Plans and Policy. (2002). Preliminary Economic Assessment, Advanced Notice of Proposed Rulemaking (ANPRM) to Add a Side Impact Test to FMVSS No. 213. http://www.nhtsa.dot.gov/cars/rules/rulings/CPSUpgrade/CPSSide/PEA/Index.html

[6] Howard A., Rothman L., McKeag M.A., Pazmino–Canizares J., German A., Monk B., Comeau J.L., Hale I., Mills D. and Blazeski S. (2003). Children in Side Impact Motor Vehicle Crashes: Seating Position and Injury Mechanism. Proceedings of the Canadian Multidisciplinary Road Safety Conference XIII, Banff, Canada.

[7] Yang X.M., Kong C.Y., Yang J.K. (2007). A Study on Accident Characteristics of Child Occupants by Passenger Car and Motorcycle in Changsha. The 5th Int. Forum of Automotive Traffic Safety (INFATS), Changsha, China.

[8] Johannsen H., Barley G., Carine S., Claeson, P., Lundell, B., Nojiri K., Renaudin, F., Rooij, L., Siewertsen, A.(2007). Review of the Development of the ISO Side Impact Test Procedure for Child Restraint Systems. 20th International Technical Conference on Enhanced Safety of Vehicles, Paper number 07-0241.

[9] Surcel MD., Gou M. (2005). Intrusion Influence on Child Occupant Behavior in the Case of a Side Impact MADYMO Simulation. ESV20th. Paper No. 05-0050.

[10] Hu J., Mizuno K. (2008). Occupant Responses in Child Restraint Systems in Side Impact Tests. Int. J. Vehicle Safety, Vol.3, No.1.

[11] Otte, D. (2003). Injury Risk of Children in Cars. 1st Conference Protection of Children in Cars, Cologne, Germany.

[12] Nagabhushana V., Morgan RM., Park J., Kuznetsov A. (2007). Impact Risk for 1-8 Year Old Children on the Struck Side in a Lateral Crash. SAE Government/Industry Meeting.

[13] Lu Y. Cao L.B., Wu J. (2008). Study on the Structural Improvement Methods for Car Side Impact Safety. China Mechanical Engineering. Vol.19 (24), (in Chinese).